

Available online at www.sciencedirect.com

ScienceDirect

www.elsevier.com/locate/jes

JES
 JOURNAL OF
 ENVIRONMENTAL
 SCIENCES
www.jesc.ac.cn

Vertical distribution of volatile organic compounds conducted by tethered balloon in the Beijing-Tianjin-Hebei region of China

Chunmei Geng¹, Jing Wang¹, Baohui Yin¹, Ruojie Zhao¹, Peng Li²,
 Wen Yang^{1,*}, Zhimei Xiao², Shijie Li¹, Kangwei Li¹, Zhipeng Bai¹

¹ State Key Laboratory of Environmental Criteria and Risk Assessment, Chinese Research Academy of Environmental Sciences, Beijing 100012, China

² Tianjin Eco-Environmental Monitoring Center, Tianjin 300191, China

ARTICLE INFO

Article history:

Received 27 September 2019

Revised 14 February 2020

Accepted 17 March 2020

Available online 4 May 2020

Keywords:

Tethered balloon

Volatile organic compounds (VOCs)

Vertical distribution

OH loss rate (L_{OH})

Ozone formation potential (OFP)

ABSTRACT

Volatile organic compounds (VOCs) as precursors of ozone and secondary organic aerosols can cause adverse effects on the environment and human health. However, knowledge of the VOC vertical profile in the lower troposphere of major Chinese cities is poorly understood. In this study, tethered balloon flights were conducted over the juncture of Beijing-Tianjin-Hebei in China during the winter of 2016. Thirty-six vertical air samples were collected on selected heavy and light pollution days at altitudes of 50–1000 meters above ground level. On average, the concentration of total VOCs (TVOCs) at 50–100 m was 4.9 times higher than at 900–1000 m (46.9 ppbV vs. 8.0 ppbV). TVOC concentrations changed rapidly from altitudes of 50–100 to 401–500 m, with an average decrease of 72%. With further altitude increase, the TVOC concentration gradually decreased. The xylene/benzene ratios of 34/36 air samples were lower than 1.1, and the benzene/toluene ratios of 34/36 samples were higher than 0.4, indicating the occurrence of aged air mass during the sampling period. Alkenes contributed most in terms of both OH loss rate (39%–71%) and ozone formation potential (40%–72%), followed by aromatics (6%–38%). Finally, the main factors affecting the vertical distributions of VOCs were local source emission and negative dispersion conditions on polluted days. These data could advance our scientific understanding of VOC vertical distribution.

© 2020 The Research Center for Eco-Environmental Sciences, Chinese Academy of Sciences. Published by Elsevier B.V.

Introduction

Jing-Jin-Ji cities have implemented various measures to prevent and control air pollution in response to the “Action plan for air pollution prevention and control” (Bai, 2014; He et al., 2013). These measures have reduced a large amount of pri-

mary air pollutant emissions to improve air quality. According to the China’s Ecological Environment Bulletin from 2015–2018 (<http://www.mee.gov.cn/hjzl/zghjzkgb/lzghjzkgb/>), the concentration of PM₁₀ (particulate matter with the aerodynamic diameter (D_p) < 10 μ m), PM_{2.5} (particulate matter with D_p < 2.5 μ m), sulphur dioxide (SO₂), nitrogen oxide (NO_x) and carbon monoxide (CO) have decreased by 17%, 22%, 47%, 6% and 40%, respectively. However, the report also indicated that the ozone (O₃) concentration increased by 23% from 2015 to 2018. Despite the improved air quality and the reduction of

* Corresponding author.

E-mail: yangwen@craes.org.cn (W. Yang).

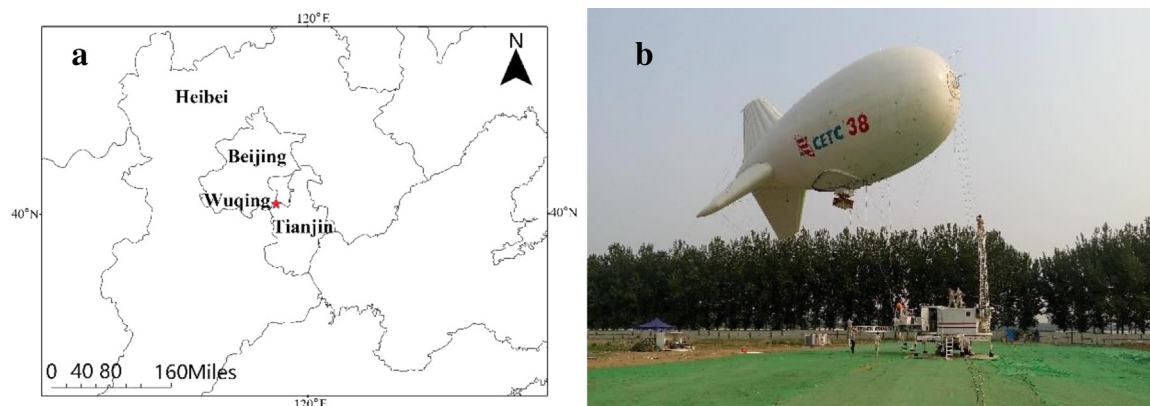


Fig. 1 – (a) Sampling site (N 39.38°, E 117.02°) in the Wuqing District of Tianjin and (b) the tethered balloon used in the study.

annual PM_{2.5} in particular, atmospheric pollution is still of major concern. In 2016, the proportion of fine days (National Standard Grade II, GB 3095-2012) in 13 cities in the Jing-Jin-Ji area was 35.8%–78.7% and the average value was 56.8%. In the winter of 2016, five widespread pollution events occurred and the highest PM_{2.5} mass concentration of over 500 µg/m³ was recorded in Beijing on December 29, 2016 (Zhu et al., 2018). As one of the main precursors of air pollution, volatile organic compounds (VOCs) contribute an important role in the formation of ozone (O₃) and secondary organic aerosols (SOA) (Barsanti et al., 2017; Hallquist et al., 2009; Sahu et al., 2017).

Many studies have measured the concentration and chemical composition of volatile organic compounds (VOCs) at ground-level (Barletta et al., 2002; Glaser et al., 2003; Shao et al., 2009; Wu et al., 2017; Venkanna, et al., 2015; Yan et al., 2017; Zhang et al., 2017a). However, knowledge of the VOC vertical profile is still poorly understood, particularly in a polluted environment. The tropospheric distribution of VOCs depends on many factors, including emission rates, dispersion, and physicochemical properties of the VOCs (Mao et al., 2008; Sangiorgi et al., 2011; Sun et al., 2018). Sun et al. (2018) found that a rapid decrease in VOC concentration appeared from the surface to an altitude of 400 m, with concentrations of alkanes, alkenes, aromatics and halocarbons decreasing by 48.0%, 53.3%, 43.3% and 51.1%, respectively, over a suburban site on the North China Plain. Yang et al. (2013) studied the effect of altitude on the distributions of VOCs from petrochemical industrial sources at ground-level and three altitudes (100, 300, and 500 m above ground-level). They found that aromatic and aliphatic compounds represented the main VOCs accounting for the maximum variance of the data observed at ground-level and high altitude. A study in suburban Beijing (Mao et al., 2008) showed that the concentrations of total VOCs (TVOCs) ranged from 51.2 ± 39.7 to 83.6 ± 44.4 ppbV on clear days and from 62.9 ± 19.0 to 105.0 ± 59.2 ppbV on hazy days. A decreasing trend in the vertical profiles up to approximately 300 m over Beijing was closely related to meteorological parameters, such as atmospheric layer stability, temperature, and wind speed.

Despite the significant effect of the VOC vertical distribution on atmospheric reactivity and chemical reaction in the lower atmosphere, few studies have been performed at different heights due to experimental difficulties. Aircraft (Reeves et al., 2010), tethered balloons (Sangiorgi et al., 2011; Zhang et al., 2018, 2019) and high towers (Deng et al., 2015; Mao et al., 2008; Sun et al., 2018) are commonly used to collect vertical samples. However, the observational level is limited by the height of the tower, which is usually less than 300 m. In ad-

dition, it is difficult to collect samples at lower altitudes (less than 1000 m) using aircraft. Tethered balloons are more flexible compared to observational towers and aircraft for vertical observations in the lower atmosphere, and can provide high resolution of vertical profiles. Some studies have qualitatively and quantitatively described the vertical distribution of VOCs using tethered balloons. Kofmann et al. (1996) reported an exponential concentration profile with altitude, and Sangiorgi et al. (2011) showed a 74%–95% reduction below the mixing layer. In addition, Zhang et al. (2018) reported that the concentration of most VOC species decreased with increased height caused by VOCs reacting with OH radical.

The Beijing-Tianjin-Hebei (Jing-Jin-Ji) region is one of the most polluted areas in China (Zhu et al., 2018). There is a lack of information describing the vertical profiles of VOCs and distribution of other air pollutants in highly polluted environments using a tethered balloon. In this study, the tethered balloon platform was used to investigate the characteristics of VOC vertical distribution in the Jing-Jin-Ji region. The main goals of the study were to (1) quantify the vertical variation of VOC concentrations and composition; (2) investigate the vertical profile of VOC reactivity; and (3) analyse the cause of different VOC vertical distributions on heavy and light pollution days.

1. Materials and methods

1.1. Field experiments

The study was performed at an open field site at Wuqing District, Tianjin, in the junction area between Beijing and Tianjin (N 39.38°, E 117.02°) shown in Fig. 1. The Beijing-Tianjin expressway was approximately 3 km southeast of the sampling site. No other obvious emission sources were nearby.

The tethered balloon platform was previously used to investigate the vertical profile of VOCs and gas pollutants in the lower troposphere in Shanghai (Zhang et al., 2017b, 2018, 2019). The balloon was filled with 1600 m³ helium and a specifically designed cable connected the balloon and the ground-level computer. The ascent and descent rates of the tethered balloon were approximately 0.5 m/sec and were controlled by an engine. The observation control platform was redesigned from previous studies and the effective capability was 200 kg.

The tethered balloon was launched on November 26 to December 19, 2016. Since the tethered balloon can only be launched when there is no rain and the wind speed is less than 10 m/sec, the sampling period was 8 days. Four air samples

Table 1 – Details of tethered balloon flights conducted in the Wuqing District of Tianjin from November 26 to December 19, 2016.

Flight No.	1	2	3	4	5	6	7	8	9
Date	November 26th	29th	30th	December 3rd	4th	13th	13th	17th	19th
Start-end Time	12:50-13:16	6:09-6:42	16:40-17:06	22:18-22:51	13:25-13:58	11:50-12:23	16:14-16:47	14:10-14:42	13:10-13:27
Sampling height (m)	100	100	100	80	80	100	200	80	50
Daily PM _{2.5} (µg/m ³)	300	200	200	300	150	300	450	300	150
	350	400	350	500	500	650	700	600	300
	790	996	770	970	1000	1000	998	950	500
	217	114	208	275	261	90	90	223	283

were collected with salinised stainless-steel canisters (3.2 L, Entech Corporation, USA) at different heights between 50–1000 m for each flight. During the field campaign, nine vertical profiles of VOCs were obtained by the tethered balloon. Detailed information for each flight is listed in Table 1. Because of the prevailing low planetary boundary layer (PBL) height (Liu et al., 2015), two or three samples were collected under 500 m. Since the altitude for sample collection was not fixed for each flight, the heights were divided into different ranges when analysing the general vertical distribution: 50–100, 101–200, 201–300, 301–400, 401–500, 501–600, 601–700, 701–800, 801–900 and 901–1000 m.

The ground-level PM_{2.5}, O₃ and meteorological parameters including temperature (T), relative humidity (RH), wind speed, and wind direction were monitored synchronously by three online instruments (Model 1405, Thermo Environmental Instruments, USA; Model 49i, Thermo Environmental Instruments, USA; WXT520, Vaisala Corporation, Finland). A ceilometer (Model CL31, Vaisala Corporation, Finland) was used to record the PBL (Eresmaa, et al., 2006).

1.2. Laboratory analysis of VOCs

VOCs were analysed by a pre-concentrator (Model 7200, Entech Instruments Inc., USA) coupled to a gas chromatograph-mass selective detector/flame ionisation detector (GC-MSD, 7890B/5977B, Agilent, USA) according to the compendium method TO-15 (methods for the determination of toxic organic compounds in ambient air). Detailed information on this method is described by the United States Environmental Protection Agency (USEPA, 1999) and has been used in previous studies (Geng et al., 2019; Liu et al., 2008a; Tsai et al., 2012; Wang et al., 2013; Yang et al., 2013; Yuan et al., 2010).

Three certified VOC standards were used for the analysis: Photochemical Assessment Monitoring Stations (PAMS, 57 compounds), TO-15 (65 compounds) and TO-14 A (internal standard, 4 compounds). All VOC standards were produced by Linde Group, North America. In total, 99 VOC species were quantified in this study. Based on functional groups, we classified these VOC species into five categories: alkanes (including cycloalkanes), alkenes, aromatics, halocarbons and oxygenated VOCs. The VOC species quantified are listed in Appendix A Table S1.

1.3. Estimation of OH loss rate and ozone formation potential

OH loss rate (L_{OH}) and ozone formation potential (OFP) were used to evaluate the reactivity of VOCs (Hui, et al., 2018; Mo, et al. 2017; Song et al., 2019; Yan et al., 2017). The L_{OH} and OFP

were calculated using the following equations:

$$L_{OH} = \sum_{i=1}^n C_i \times k_{OH, i} \quad (1)$$

$$OFP = \sum_{i=1}^n C_i \times MIR_i \quad (2)$$

where C_i is the mass concentration of species i ; $k_{OH, i}$ is the OH rate constant of species i ; and MIR_i is the maximum incremental reactivity (MIR) value of species i , as cited by Carter (2010).

2. Results and discussion

2.1. Pollution and meteorological conditions at the ground-level

The variation of ground-level PM_{2.5} and O₃ concentrations, and the meteorological parameters recorded during the field campaign are shown in Fig. 2. Several PM_{2.5} processes were observed in the region during the field campaign. PM_{2.5} was the main pollutant detected. As identified previously, unfavourable weather conditions were the main factor affecting the accumulation of pollutants (Sun et al., 2016, 2018; Zhu et al., 2018). Specifically, the low temperature (3.5°C on average), high humidity (68% on average) and low wind speed (1.05 m/sec on average) did not favour the diffusion of pollutants. Additionally, the atmospheric oxidation capacity at the ground-level was low, which was reflected by the average O₃ concentration of 13 µg/m³.

To investigate the characteristics of VOCs under different pollution conditions, sampling days were divided into light pollution days and heavy pollution days. According to the Chinese National Ambient Air Quality Standard, days on which the PM_{2.5} exceeds 75 µg/m³ (Grade II) are defined as polluted. We used the PM_{2.5} value of 150 µg/m³ (a 2-fold Grade II standard value) to separate light pollution and heavy pollution days. Based on this, the study sampled two light pollution days and six heavy pollution days.

2.2. Vertical distribution of VOCs

Fig. 3 shows the average vertical profiles of TVOC, as well as the proportion of each VOC category. Generally, the TVOC concentrations decreased with increased altitude, as previously observed (Mao et al., 2008; Sun et al., 2018; Xue et al., 2011). The ground-level TVOC concentrations were 4.9 times higher than at 900–1000 m (46.9 ppbV vs. 8.0 ppbV). The average TVOC concentration measured at 400–500 m decreased by 72%. In the 50–500 m range, the concentrations of alkanes, alkenes, aromatics, halocarbons and oxygenated VOCs

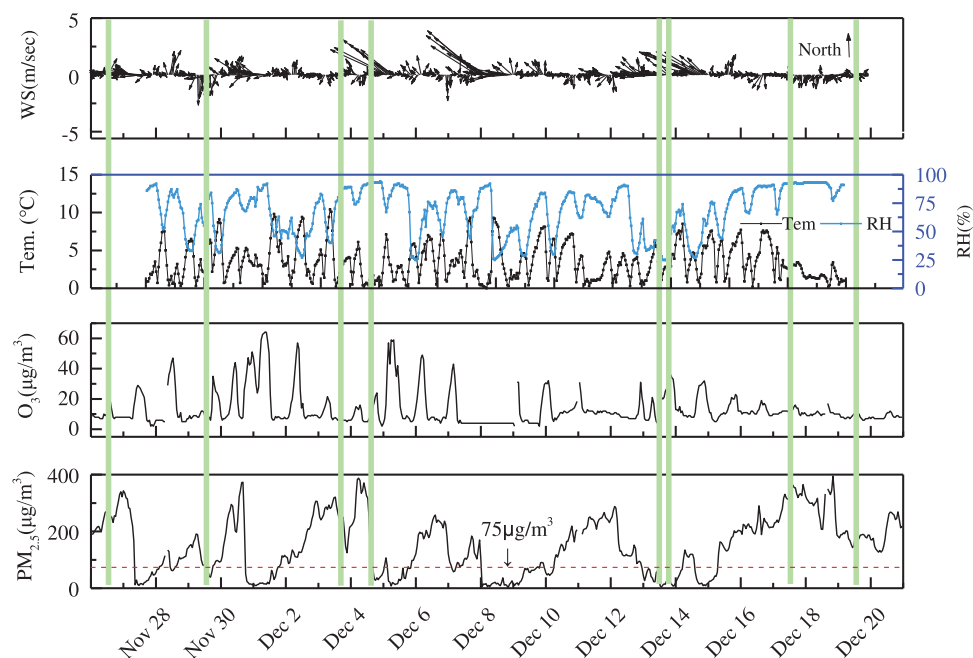


Fig. 2 – Variation of ground-level PM_{2.5} (particulate matter with the aerodynamic diameter (D_p) < 2.5 μm) and ozone (O_3) as well as meteorological parameters during the study. The light green bar represents flight period; 75 $\mu\text{g}/\text{m}^3$ is the Grade II limit for the PM_{2.5} daily average stated by the Chinese National Ambient Air Quality Standard (GB 3096-2012). WS: wind speed; Tem.: temperature; RH: relative humidity.

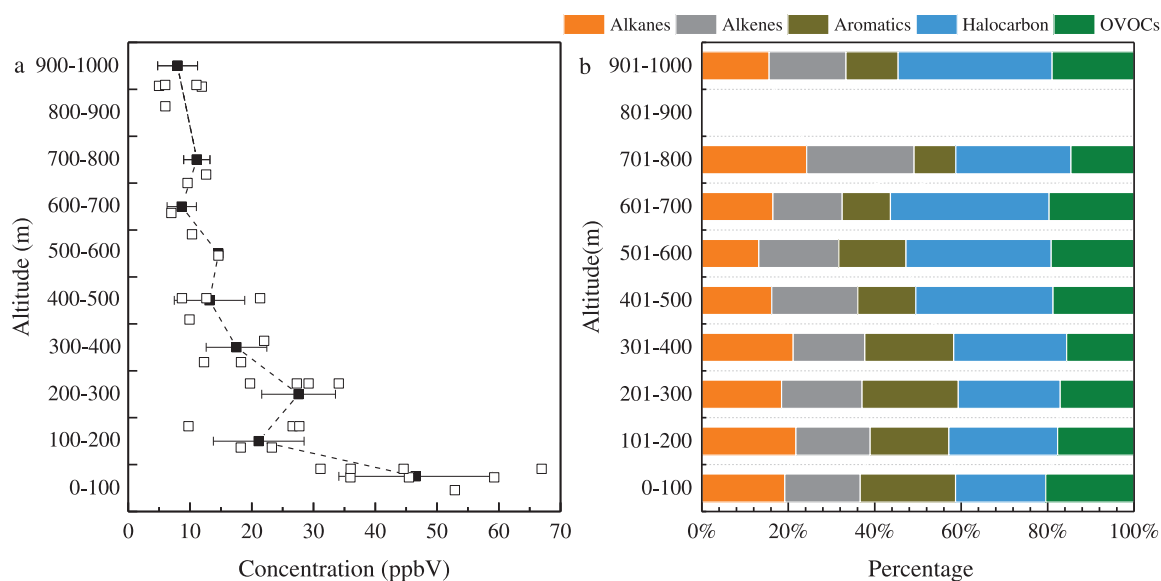


Fig. 3 – Vertical profile of (a) total volatile organic compound (TVOC) concentrations and (b) the proportion of each VOC category at different height ranges. OVOCs: oxygenated volatile organic compounds.

(OVOCs) decreased by 76%, 69%, 83%, 57% and 74%, respectively. Between 500–1000 m, the concentrations of aromatics declined by 57%; alkenes, halocarbon and OVOCs decreased by 47%, 42% and 46%, respectively; and alkanes decreased by 35%. Additionally, there was a peak at 200–300 m in TVOC concentration, which indicated the existence of an inversion layer. Another study found that the inversion layer occurred at 400 m above ground-level using a tethered balloon in Berlin (Glaser et al., 2003).

The PBL height is an important meteorological factor that affects the accumulation and vertical diffusion of atmospheric pollutants (Ren et al., 2004; Tang et al., 2016; Zhu et al., 2018). As reported by Zhu et al. (2018), the estimated PBL height was ~ 870 m at 14:00 (Beijing Time) and the monthly average was ~ 280 m during December 2016 in the Jing-Jin-Ji region. The PBL height obtained by ceilometer in this study was similar to Zhu's study (Zhu et al., 2018). The daily variations of PBL on a light pollution day (December 13, 2016)

Table 2 – Concentrations, OH loss rate (L_{OH}) and ozone formation potential (OFP) for selected abundant species and TVOCs at different heights on heavy and light pollution days.

	Species	Heavy pollution days			Light pollution days		
		50-200 m (n = 9)	300-500 m (n = 9)	600-1000 m (n = 6)	50-200 m (n = 4)	300-500 m (n = 3)	501-1000 m (n = 5)
Concentration (ppbV)	Propene	3.8	2.0	0.9	3.6	0.9	0.9
	1-Butene	2.1	1.5	1.0	1.4	0.6	0.3
	Iso-butane	1.6	0.9	0.4	1.2	0.7	0.3
	Butane	2.2	1.3	0.6	2.1	1.5	0.7
	Chloromethane	1.0	0.8	0.7	0.9	0.8	0.5
	Methylene chloride	3.0	1.5	0.6	2.0	1.3	0.7
	Benzene	2.9	1.7	0.5	2.0	1.1	0.5
	Toluene	3.0	1.2	0.3	1.8	0.4	0.3
	Acetone	1.3	1.0	0.7	1.0	0.8	0.6
	Ethyl acetate	3.4	1.1	0.3	2.0	0.8	0.4
Sum of the above 10 species	24.3	12.9	5.8	18.1	8.8	5.2	
OFP (ppbV)	TVOCs	40.6	20.5	9.7	28.3	16.5	9.1
	Propene	44.9	23.3	10.4	42.6	10.2	10.8
	1-Butene	20.0	14.5	9.4	13.6	5.9	3.1
	m-Xylene	13.1	3.8	0.8	8.4	1.8	1.9
	Toluene	12.2	4.7	1.2	7.4	1.4	1.0
	trans-2-Butene	4.0	4.5	2.7	3.6	2.2	0.6
	p-Xylene	3.2	1.0	0.3	1.7	0.4	0.4
	Butane	2.5	1.5	0.7	2.4	1.7	0.8
	Ethyl acetate	2.1	0.7	0.2	1.3	0.5	0.2
	Benzene	2.1	1.2	0.3	1.4	0.8	0.3
L_{OH} (sec ⁻¹)	Isobutane	2.0	1.1	0.5	1.5	0.9	0.4
	Sum of the above 10 species	106.0	56.2	26.5	83.7	25.9	19.7
	TVOCs	133.1	69.1	33.6	104.1	48.0	26.8
	Propene	2.40	1.25	0.56	2.28	0.55	0.58
	1-Butene	1.53	1.11	0.72	1.04	0.46	0.24
	m-Xylene	0.75	0.21	0.05	0.48	0.10	0.11
	Toluene	0.41	0.16	0.04	0.25	0.05	0.03
	trans-2-Butene	0.40	0.45	0.27	0.36	0.22	0.06
	Octane	0.24	0.05	0.01	0.15	0.03	0.02
	1,3-Butadiene	0.19	0.05	0.02	0.34	0.22	0.10
p-Xylene	0.19	0.06	0.02	0.10	0.02	0.03	
cis-2-Butene	0.17	0.07	0.06	0.18	0.08	0.03	
Styrene	0.17	0.14	0.03	0.12	0.10	0.04	
Sum of the above 10 species	6.45	3.54	1.76	5.29	1.83	1.25	
TVOCs	8.85	4.89	2.49	7.12	3.95	1.96	

Heavy pollution days ($75 \mu\text{g}/\text{m}^3 < \text{PM}_{2.5} \leq 150 \mu\text{g}/\text{m}^3$): November 26, November 30, December 3, December 4, December 17 and December 19.
Light pollution days ($\text{PM}_{2.5} > 150 \mu\text{g}/\text{m}^3$): November 29 and December 13.

and a heavy pollution day (December 4, 2016) are shown in Appendix A Fig. S1. A low PBL height inhibited the air convection and caused ground air pollution. Considering the low PBL height, the high TVOC concentration in the lower atmosphere was partly due to local emission and the stable atmospheric structure near ground-level. Compared with near ground-level, the concentration of TVOCs decreased sharply at 300-400 m. As the height increased further, the vertical dilution made the pollutant mix more evenly and the horizontal dispersion conditions improved. As a result, the TVOC concentration decreased slowly in the upper atmosphere, especially for the alkanes and halocarbons that have relatively low reactivity.

To further examine the characteristics of VOC vertical distribution, the concentrations of VOCs on heavy and light pollution days were separated for analysis. According to the monthly PBL average of 280 m (Zhu et al., 2018), sampling height was divided into three ranges: 50-200, 300-500 and 501-1000 m. In general, there was no significant difference in the

fingerprint of VOCs on heavy and light pollution days, which indicated that pollutants from local emission sources might be the main constituent. Table 2 lists the concentrations of ten abundant VOC species at different altitudes on heavy and light pollution days. The ten VOC species with high concentrations accounted for 60%-63% of the TVOCs on heavy pollution days and 53%-64% of the TVOCs on light pollution days. Due to the high concentration near ground-level, VOC concentrations on heavy pollution days were higher than on light pollution days at nearly every altitude sampled. As the altitude increased, the concentration of each VOC decreased. This data demonstrated that the VOC concentrations peaked at the ground surface and decreased with altitude, which is similar to previous reports (Mao et al., 2008; Sangiorgi et al., 2011; Xue et al., 2011).

2.3. VOC vertical profile: light vs. heavy polluted days

Two days were selected to illustrate the vertical characteristics of VOCs and meteorological conditions. One day was associ-

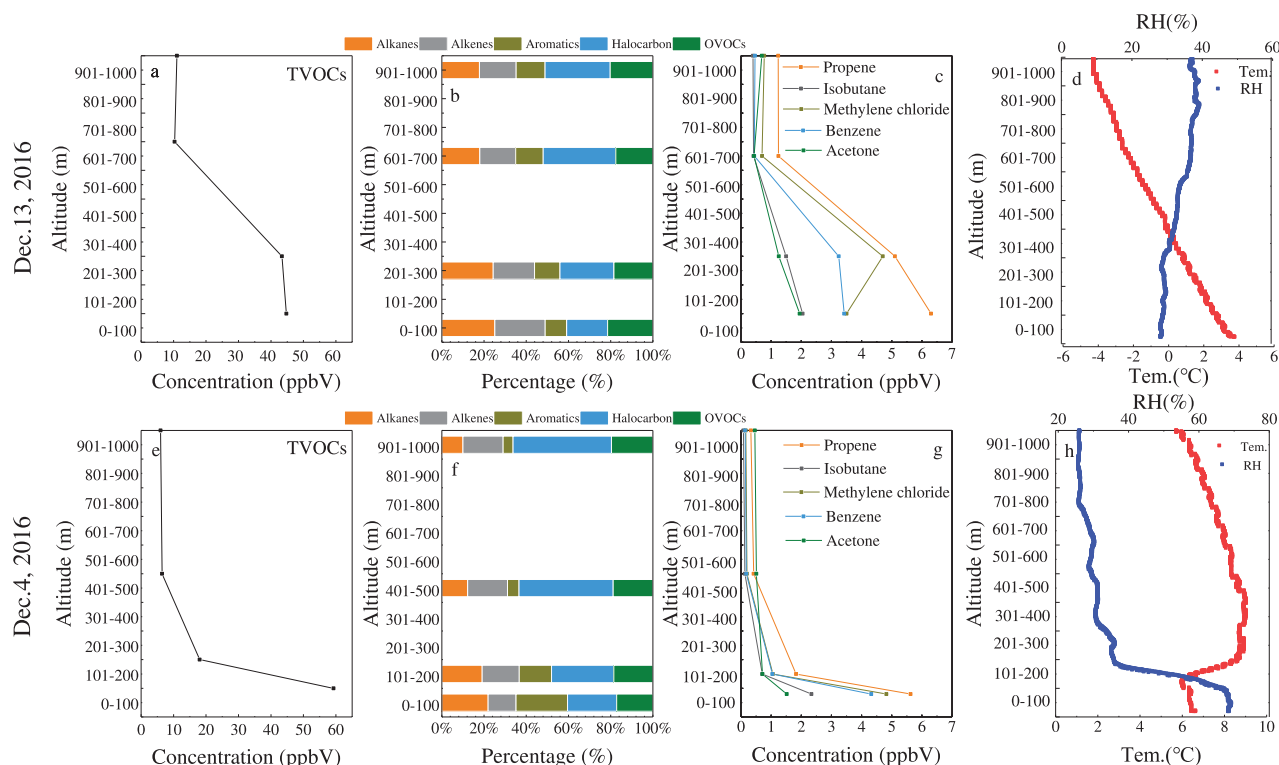


Fig. 4 – Vertical profile of TVOC, selected VOC species, proportion of VOC category, and meteorological conditions (temperature and relative humidity) at noon for two selected flights. (a), (b), (c) and (d) are the result on December 13, 2016 (11:50-12:23, $PM_{2.5} = 90 \mu\text{g}/\text{m}^3$); (e), (f), (g) and (h) are the result on December 4, 2016 (13:25-13:58, $PM_{2.5} = 261 \mu\text{g}/\text{m}^3$).

ated with a light pollution day ($PM_{2.5} = 90 \mu\text{g}/\text{m}^3$) on December 13, 2016, and the other day was classified as a heavy pollution day ($PM_{2.5} = 261 \mu\text{g}/\text{m}^3$) on December 4, 2016. On both days, sampling was performed at noon. The spatial distribution of the primary pollutant $PM_{2.5}$ on the light and heavy polluted days had regional characteristics, as shown in Appendix A Fig. S2. Iso-butane, propene, benzene, methylene chloride and acetone were selected as abundant representative compounds in the categories of alkanes, alkenes, aromatics, halocarbons and OVOCs, respectively. Each compound was expected to provide the typical distribution for its category.

As shown in Fig. 4, the temperature increased sharply with increasing altitude from 130 to 280 m and then slowly increased until an altitude of 400 m on the heavy pollution day (13:25-13:58, December 4, 2016). The temperature then decreased with increasing altitude. Ceilometer data showed there was a mixing height at approximately 140 m at noon on December 4, 2016 (Appendix A Fig. S1); therefore, there was a significant inversion layer at 130-140 m. Although the time was 13:25, it appeared that the pollutants were prohibited from diffusion in the upper atmosphere. The TVOC decreased sharply at 80 m (TVOC = 59.3 ppbV) to 150 m (TVOC = 18.0 ppbV). At higher altitudes, the sampling was above the inversion layer; here, the TVOC concentrations were 6.5 ppbV at 500 m and 6.0 ppbV at 1000 m. The concentrations of iso-butane, propene, benzene, methylene chloride and acetone reduced with increasing altitude, similar to that of TVOC concentration. Compared with the concentration at 80 m, the reduction rate was more than 53% at 150 m and more than 70% at 1000 m.

The vertical distribution on the light pollution day (December 13, 2016) showed a different pattern. In this case, the temperature decreased and relative humidity gradually increased

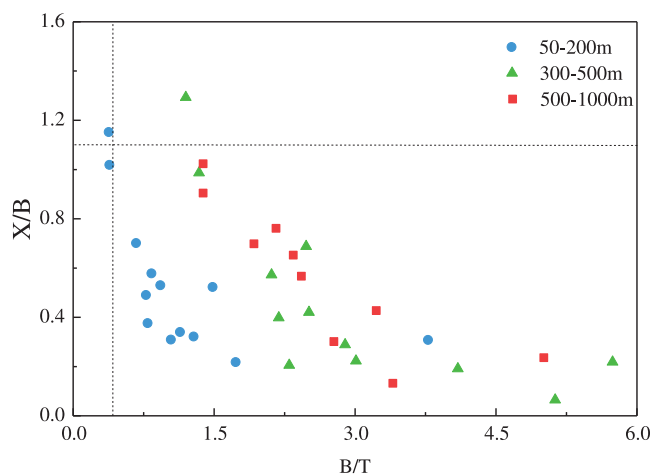


Fig. 5 – Aging extent assessment of air mass using X/B (xylene/benzene) and B/T (benzene/toluene) ratios at different heights 50-200, 300-500 and 500-1000 m.

at elevated heights when vertical monitoring was conducted at noon (11:50-12:23, December 13, 2016). This phenomenon was consistent with the change of PBL. In the morning, the ground was heated by sunlight, leading to the collapse of the boundary layer at noon (Appendix A Fig. S1). Thus, the vertical dispersion condition was favourable for the diffusion of pollutants. The TVOC concentrations decreased from 44.7 ppbV at 100 m to 11.0 ppbV at 1000 m. Good diffusion conditions contributed to the high concentration at low altitude so that

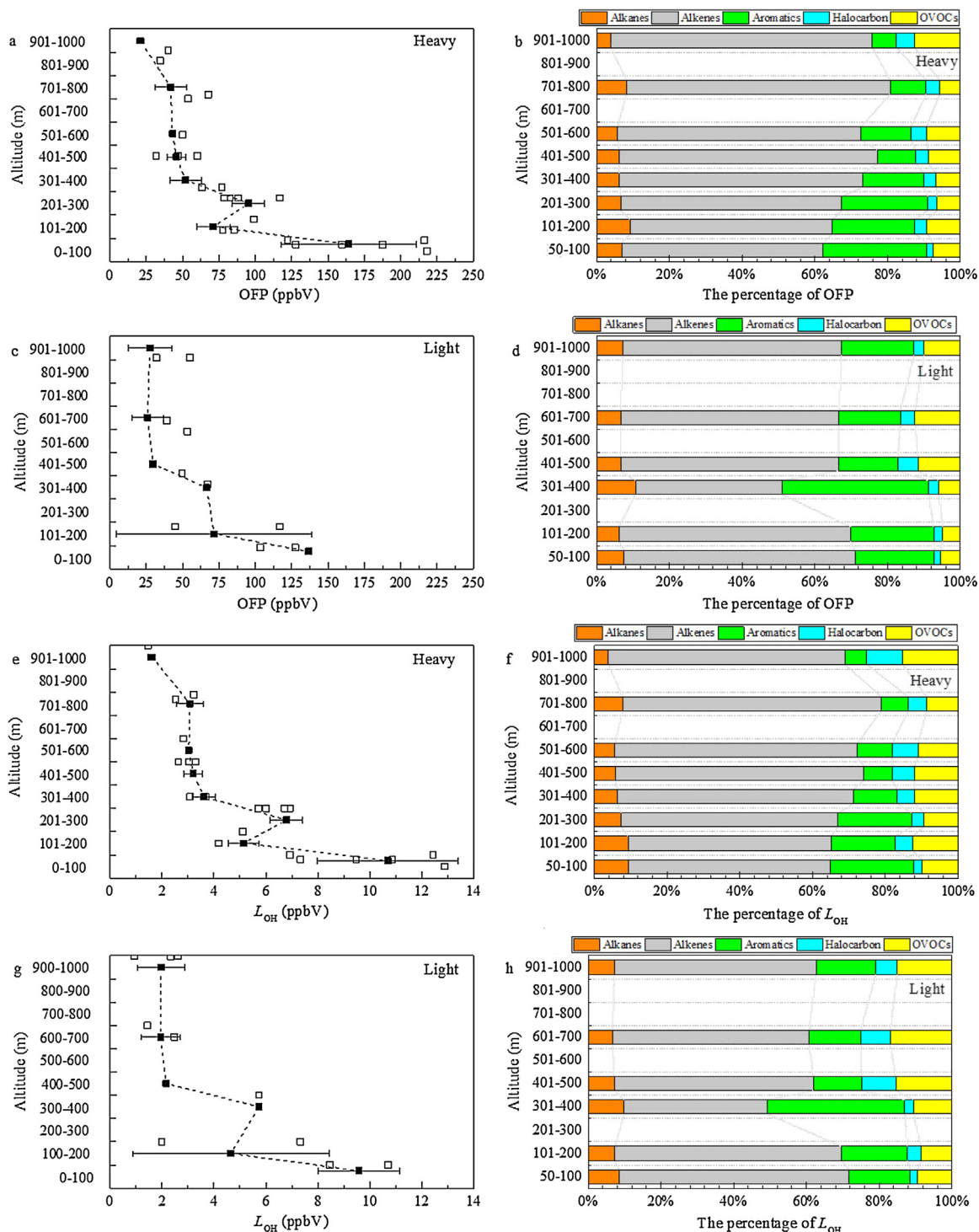


Fig. 6 – Vertical profiles of ozone formation potential (OFP) and OH loss rate (L_{OH}) during heavy and light pollution days. (a), (c), (e) and (g) are the vertical profiles of OFP or L_{OH} of TVOCs, and (b), (d), (f) and (h) are the vertical profile of the proportion of each VOC category in the OFP or L_{OH} of TVOCs.

the TVOCs (43.4 ppbV) at 300 m was similar to that at 100 m. However, at higher altitude (650 m), TVOC concentration decreased to 10.0 ppbV. In general, the compound concentration decreased as the altitude increased. The acetone concentration decreased by 36% as the altitude increased from 100 to 300 m, which represented the greatest decreasing rate from

compounds tested. For the other compounds, the decreasing rate was less than 27%. At 1000 m, the largest concentration reduction was 86% for benzene and the lowest concentration reduction was 64% for acetone.

The vertical distributions of VOCs are affected by many factors, such as source emission, meteorological parameters, and

photochemical reactions (Mao et al., 2008; Zhu et al., 2018). The representative compounds measured are from anthropogenic emissions: propene is from vehicle emissions (Liu et al., 2008a); iso-butane is from liquefied petroleum gas evaporation and oil refinery (Liu et al., 2008a); methylene chloride is a form of organic solvent and mainly released from solvent evaporation (Mao et al., 2008); benzene comes from vehicular and gasoline vapour emissions (Liu et al., 2008a; Song et al., 2007); and acetone was the predominant ambient VOC species detected at a petrochemical complex and an oil refinery (Cetin et al., 2003). In the present study, no significant difference was seen in the chemical composition and concentration of samples near ground-level on heavy or light pollution days, indicating that stable emission sources existed in the studied area. The vertical profile of five representative compounds on light pollution days was more dispersive than on heavy pollution days, which reflect the effect of vertical convective dispersion conditions and the reactivity of compounds (Mao et al., 2008).

2.4. Aged air parcel assessment

Based on the estimation of photochemical reactivity, ratios of two VOC species have commonly been used to identify the VOC sources and chemical evolution (Geng et al., 2019; Parrish et al., 2007; Yuan et al., 2012a, 2012b). For example, benzene, toluene and xylene have been used as indicators of air mass age and vehicular exhaust emissions (Baldasano et al., 1998; Monod et al., 2001; Song et al., 2007; Sweet and Vermette, 1992). Due to the different reaction rate, low X/B (xylene/benzene) and high B/T (benzene/toluene) ratios were used to identify the aged air mass. Previous studies suggested that a fresh air-mass sample could be identified when the B/T ratio was < 0.4 and the X/B ratio was > 1.1 , and an aged air parcel could be identified when the B/T ratio was ≥ 0.4 and the X/B ratio was ≤ 1.1 (Liu et al., 2008b; Vo et al., 2018). Fig. 5 shows the degree of air mass ageing using X/B (xylene/benzene) and B/T (benzene/toluene) ratios at different heights. The X/B ratios of 34/36 air samples were lower than 1.1, and the B/T ratios of 34/36 samples were higher than 0.4, indicating the occurrence of aged air mass during the sampling period. The temperature and wind speed were low during winter, resulting in weak diffusion conditions. Combined with the barrier effect of low PBL, the pollutants remained in the atmosphere for a relatively long time. Thus, fresh air was rarely collected.

It has been reported that a B/T ratio in the range of 0.2-1.5 is an indicator of traffic source emission (Garzon et al., 2015). We found that most samples (11 from 13) from 50-200 m were within a B/T ratio of 0.2-1.5, indicating that local vehicular exhaust was an important source. The vehicular emission from the Beijing-Tianjin expressway located southeast of the sampling site might be an important source.

The ratios of B/T and X/B varied widely (Appendix A Fig. S3). On the heavy pollution day, X/B decreased with increasing altitude and B/T increased with increasing altitude, indicating an aged trend at the upper heights. These aged air masses above the inversion layer could have originated from local mobile and stationary emissions as well as transportation from distant sources. For the light pollution day, there was no variation in the X/B and B/T ratios. Therefore, it was confirmed that diffusion was an important factor for the mass ageing process.

2.5. Vertical profile of VOC reactivity

OH loss rate (L_{OH}) and ozone formation potential (OFP) were used to evaluate the vertical profile of VOC reactivity. Fig. 6 shows the L_{OH} and OFP of TVOCs and each VOC group at different altitudes on heavy and light pollution days.

On heavy pollution days, the average L_{OH} and OFP for TVOCs were 10.70 sec^{-1} and 164.1 ppbV near ground-level, re-

spectively. They decreased sharply from near ground level to 300-400 m, with a L_{OH} reduction ratio of 66% and an OFP reduction ratio of 68%. At altitudes above 300 m, the L_{OH} and OFP level changed slowly. On light pollution days, the L_{OH} and OFP for TVOCs were 9.58 sec^{-1} and 136.6 ppbV near ground-level, respectively, which were slightly lower than on heavy pollution days. The variation of L_{OH} and OFP above 400 m was small. On the heavy and light pollution days, alkenes contributed most in terms of L_{OH} (39%-71%) and OFP (40%-72%), followed by aromatics (6%-38%). A study conducted in the lower troposphere in Shijiazhuang, Hebei province, also found that alkenes and aromatics were the main contributors to ozone formation (Sun et al., 2018).

Table 2 lists ten abundant species in L_{OH} and OFP, as well as the L_{OH} and OFP of TVOCs at different altitudes on heavy and light pollution days. The abundant species for L_{OH} and OFP differed compared to the VOC concentration. The ten selected reactive species accounted for 46%-74% and 54%-81% of the L_{OH} and OFP for TVOCs, respectively. The 10 species and their concentrations were similar between heavy and light pollution days, indicating that the types of emission sources were relatively constant during the sampling period.

3. Conclusions

In this study, a tethered balloon platform was used to investigate the characteristics of VOC vertical distribution over the Jing-Jin-Ji region: one of the most highly polluted areas in China. The tethered balloon was launched from ~ 50 to ~ 1000 m between November 26 and December 19, 2016. Four air samples were collected at different heights for each flight, and nine VOC vertical profiles were obtained. During the sampling period, low temperature, high humidity and low wind speed at ground-level were not favourable to the dispersion of pollutants.

In general, the TVOC concentration decreased with increasing altitude, and the TVOC concentration near ground-level (50-100 m) was 4.9 times higher than that at 900-1000 m (46.9 ppbV vs. 8.0 ppbV). The vertical variation of TVOCs decreased by 72% from altitudes of 50-100 to 401-500 m. The high TVOC concentration at a lower atmosphere was attributed to local emission and the stagnant atmospheric structure near ground-level (below the boundary layer). Propene, 1-butene, iso-butane, butane, benzene, toluene and ethyl acetate species had the highest concentration, OFP and L_{OH} . Based on X/B and B/T ratios, almost all samples were identified as aged air mass. The air mass showed an ageing trend at the upper altitudes. Alkenes and aromatics were identified as the main contributors to the total L_{OH} and OFP on heavy and light pollution days. In summary, these results can contribute to our scientific understanding of VOC vertical distribution over the Jing-Jin-Ji region in China.

Declaration of competing interest

The authors declare that they have no known competing financial interests or personal relationships that could have appeared to influence the work reported in this paper.

Acknowledgments

This work was supported by the Natural Science Foundation of China (No. 41275135), National science and technology support program (No. 2014BAC23B01), the National Key Research

and Development Plan (No. 2017YFC0212503) and Central - level public welfare research institutes Basic research special funding (No. CRAES 2018-041).

Appendix A. Supplementary data

Supplementary material associated with this article can be found in the online version at doi:10.1016/j.jes.2020.03.026.

REFERENCES

- Bai, C.L., 2014. Progress and prospect on atmospheric haze research in Chinese Academy of Sciences. *CAS Bulletin* 29 (3), 275–281.
- Baldasano, J.M., Delgado, R., Calbo, J., 1998. Applying receptor models to analyze urban/suburban VOCs air quality in Martorell (Spain). *Environ. Sci. Technol.* 32, 405–412.
- Barletta, B., Meinardi, S., Simpson, I.J., Khwaja, H.A., Blake, D.R., Rowland, F.S., 2002. Mixing ratios of volatile organic compounds (VOCs) in the atmosphere of Karachi, Pakistan. *Atmos. Environ.* 36, 3429–3443.
- Barsanti, K.C., Kroll, J.H., Thornton, J.A., 2017. Formation of low-volatility organic compounds in the atmosphere: Recent advancements and insights. *J. Phys. Chem. Lett.* 8, 1503–1511.
- Carter, W.P.L., 2010. Development of the SAPRC-07 chemical mechanism. *Atmos. Environ.* 44, 5324–5335.
- Cetin, E., Odabasi, M., Seyfioglu, R., 2003. Ambient volatile organic compound (VOC) concentrations around a petrochemical complex and a petroleum refinery. *Sci. Total Environ.* 312, 103–112.
- Deng, X., Li, F., Li, Y., Li, J., Huang, H., Liu, X., 2015. Vertical distribution characteristics of PM in the surface layer of Guangzhou. *Particuology* 20, 3–9.
- Eresmaa, N., Karppinen, A., Joffre, S., Rasanen, M.J., Talvitie, H., 2006. Mixing height determination by ceilometer. *Atmos. Chem. Phys.* 6, 1485–1493.
- Garzon, J.P., Huertas, J.I., Magana, M., Huertas, M.E., Cardenas, B., Watanabe, T., et al., 2015. Volatile organic compounds in the atmosphere of Mexico City. *Atmos. Environ.* 119, 415–429.
- Geng, C., Yang, W., Sun, X.S., Wang, X.H., Bai, Z.P., Zhang, X., 2019. Emission factors, ozone and secondary organic aerosol formation potential of volatile organic compounds emitted from industrial biomass boilers. *J. Environ. Sci.* 83, 64–72.
- Glaser, K., Vogt, U., Baumbach, G., Volz-Thomas, A., Geiss, H., 2003. Vertical profiles of O₃, NO₂, NOx, VOC, and meteorological parameters during the Berlin ozone experiment (BERLIOZ) campaign. *J. Geophys. Res.* 108, 8253–8266.
- Hallquist, M., Wenger, J.C., Baltensperger, U., Rudich, Y., Simpson, D., Claeys, M., et al., 2009. The formation, properties and impact of secondary organic aerosol: Current and emerging issues. *Atmos. Chem. Phys.* 9, 5155–5236.
- He, H., Wang, X.M., Wang, Y.S., Wang, Z.F., Liu, J.G., Chen, Y.F., 2013. Formation mechanism and control strategies of haze in China. *CAS Bulletin* 28 (3), 344–352.
- Hui, L., Liu, X., Tan, Q., Feng, M., An, J., Qu, Y., et al., 2018. Characteristics, source apportionment and contribution of VOCs to ozone formation in Wuhan, Central China. *Atmos. Environ.* 192, 55–71.
- Koßmann, M., Vogel, H., Vogel, B., Vögtlin, R., Corsmeier, U., Fiedler, F., et al., 1996. The composition and vertical distribution of hydrocarbons in southwestern Germany, eastern France and Northern Switzerland during the TRACT campaign in September 1992. *Phys. Chem. Earth* 21, 429–433.
- Liu, L.W., Li, W.C., Shang, K.Z., Wang, S.G., Chu, J.H., Fu, J., 2015. Analysis of a serious haze process and its impact factors in Jing-jin-ji region. *J. Meteor. Environ.* 31, 35–42.
- Liu, Y., Shao, M., Fu, L.L., Lu, S.H., Zeng, L.M., Tang, D.G., 2008a. Source profiles of volatile organic compounds (VOCs) measured in China: part 1. *Atmos. Environ.* 42, 6247–6260.
- Liu, P., Yao, Y., Tsai, J., Hsu, Y., Chang, L., Chang, K., 2008b. Source impacts by volatile organic compound in an industrial city of southern Taiwan. *Sci. Total Environ.* 398, 154–163.
- Mao, T., Wang, Y.S., Jiang, J., Wu, F.K., Wang, M., 2008. The vertical distributions of VOCs in the atmosphere of Beijing in autumn. *Sci. Total Environ.* 390, 97–108.
- Mo, Z., Shao, M., Lu, S., Niu, H., Zhou, M., Sun, J., 2017. Characterization of non-methane hydrocarbons and their sources in an industrialized coastal city, Yangtze River Delta, China. *Sci. Total Environ.* 593–594, 641–653.
- Monod, A., Sive, C.S., Avino, P., Chen, T., Blake, D.R., Rowland, S., 2001. Monoaromatic compounds in ambient air of various sites: a focus on correlations between the xylenes and ethylbenzene. *Atmos. Environ.* 35, 135–149.
- Parrish, D.D., Stohl, A., Forster, C., Atlas, E.L., Blake, D.R., Goldan, P.D., 2007. Effects of mixing on evolution of hydrocarbon ratios in the troposphere. *J. Geophys. Res.: Atmos.* 112, D10S34.
- Reeves, C.E., Formenti, P., Afif, C., Ancellet, G., 2010. Chemical and aerosol characterization of the troposphere over West Africa during the monsoon period as part of AMMA. *Atmos. Chem. Phys.* 10, 7575–7601.
- Ren, Z.H., Wan, B.T., Tong, Y.U., Su, F.Q., Zhang, Z.G., Gao, Q.X., et al., 2004. Influence of weather system of different scales on pollution boundary layer and the transport in horizontal current field. *Res. Environ. Sci.* 17 (1), 7–13.
- Sahu, L.K., Tripathi, N., Yadav, R., 2017. Contribution of biogenic and photochemical sources to ambient VOCs during winter to summer transition at a semi-arid urban site in India. *Environ. Pollut.* 229, 595–606.
- Sangiorgi, G., Ferrero, L., Perrone, M.G., Bolzacchini, E., Duane, M., Larsen, B.R., 2011. Vertical distribution of hydrocarbons in the low troposphere below and above the mixing height: tethered balloon measurements in Milan, Italy. *Environ. Pollut.* 159, 3545–3552.
- Shao, M., Zhang, Y., Zeng, L., Tang, X., Zhang, J., Zhong, L., et al., 2009. Ground level ozone in the Pearl River delta and the roles of VOC and NOx in its production. *J. Environ. Manag.* 90, 512–518.
- Song, M., Liu, X., Zhang, Y., Shao, M., Lu, K., Tan, Q., et al., 2019. Sources and abatement mechanisms of VOCs in southern China. *Atmos. Environ.* 201, 28–40.
- Song, Y., Shao, M., Liu, Y., Lu, S.H., Kuster, W., Goldan, P., et al., 2007. Source apportionment of ambient volatile organic compounds in Beijing. *Environ. Sci. Technol.* 41, 4348–4353.
- Sun, J., Wang, Y.S., Wu, F.K., Tang, G.Q., Wang, L.L., Wang, Y.H., et al., 2018. Vertical characteristics of VOCs in the lower troposphere over the North China Plain during pollution periods. *Environ. Pollut.* 236, 907–915.
- Sun, J., Wu, F., Hu, B., Tang, G., Wang, Y., 2016. VOC characteristics, emissions and contributions to SOA formation during hazy episodes. *Atmos. Environ.* 141, 560–570.
- Sweet, C., Vermette, S., 1992. Toxic volatile organic compounds in urban air in Illinois. *Environ. Sci. Technol.* 26, 165–173.
- Tang, G., Zhang, J., Zhu, X., Song, T., Munkel, C., Hu, B., et al., 2016. Mixing layer height and its implications for air pollution over Beijing, China. *Atmos. Chem. Phys.* 16, 2459–2475.
- Tsai, H.H., Liu, Y.F., Yuan, C.S., Chen, W.H., Lin, Y.C., Hung, C.H., et al., 2012. Vertical profile and spatial distribution of ozone and its precursors at the inland and offshore of an industrial city. *Aerosol Air Qual. Res.* 12, 911–922.
- USEPA, 1999. Compendium of Methods for the Determination of Toxic Organic Compounds in Ambient Air, TO-15.
- Venkanna, R., Nikhil, G.N., Sinha, P.R., Rao, T.S., Swamy, Y.V., 2015. Significance of volatile organic compounds and oxides of nitrogen on surface ozone formation at semi-arid tropical urban site, Hyderabad, India. *Air Qual. Atmos. Health.* 9, 379–390.
- Vo, T., Lin, C.S., Weng, C.E., Yuan, C.S., Lee, C.W., Hung, C.H., et al., 2018. Vertical stratification of volatile organic compounds and their photochemical product formation potential in an industrial urban area. *J. Environ. Manag.* 217, 327–336.
- Wang, Q., Geng, C., Lu, S., Chen, W., Shao, M., 2013. Emission factors of gaseous carbonaceous species from residential combustion of coal and straw briquettes. *Front. Environ. Sci. Eng.* 7 (1), 66–76.
- Wu, W., Zhao, B., Wang, S., Hao, J., 2017. Ozone and secondary organic aerosol formation potential from anthropogenic volatile organic compounds emissions in China. *J. Environ. Sci.* 53, 224–237.
- Xue, L., Wang, T., Simpson, I.J., Ding, A., Gao, J., Blake, D.R., et al., 2011. Vertical distributions of non-methane hydrocarbons and halocarbons in the lower troposphere over Northeast China. *Atmos. Environ.* 45, 6501–6509.
- Yan, Y., Peng, L., Li, R., Li, Y., Li, L., Bai, H., 2017. Concentration, ozone formation potential and source analysis of volatile organic compounds (VOCs) in a thermal power station centralized area: a study in Shuozhou, China. *Environ. Pollut.* 223, 295–304.
- Yang, J.J., Liu, C.C., Chen, W.H., Yuan, C.S., Lin, C., 2013. Assessing the altitude effect on distributions of volatile organic compounds from different sources by principal component analysis. *Environ. Sci.: Processes Impacts* 15, 972–985.
- Yuan, B., Chen, W.T., Shao, M., Wang, M., Lu, S.H., Wang, B., et al., 2012a. Measurements of ambient hydrocarbons and carbonyls in the Pearl River Delta (PRD), China. *Atmos. Res.* 116, 93–104.
- Yuan, B., Shao, M., Gouw, J.D., Parrish, D.D., Lu, S.H., Wang, M., et al., 2012b. Volatile organic compounds (VOCs) in urban air: How chemistry affects the interpretation of positive matrix factorization (PMF) analysis. *J. Geophys. Res.* 117, D24302.
- Yuan, B., Shao, M., Lu, S., Wang, B., 2010. Source profiles of volatile organic compounds associated with solvent use in Beijing, China. *Atmos. Environ.* 44, 1919–1926.
- Zhang, Z., Wang, H., Chen, D., Li, Q., Thai, P., Gong, D., et al., 2017a. Emission characteristics of volatile organic compounds and their secondary organic aerosol formation potentials from a petroleum refinery in Pearl River Delta, China. *Sci. Total Environ.* 584, 1162–1174.
- Zhang, K., Wang, D.F., Bian, Q.G., Duan, Y.S., Zhao, M.F., Fei, D.N., et al., 2017b. Tethered balloon-based particle number concentration, and size distribution vertical profiles within the lower troposphere of Shanghai. *Atmos. Environ.* 154, 141–150.
- Zhang, K., Xiu, G.L., Zhou, L., Bian, Q.G., Duan, Y.S., Fei, D.N., et al., 2018. Vertical distribution of volatile organic compounds within the lower troposphere in late spring of Shanghai. *Atmos. Environ.* 186, 150–157.
- Zhang, K., Zhou, L., Fu, Q.Y., Yan, L., Bian, Q.G., Wang, D.F., et al., 2019. Vertical distribution of ozone over Shanghai during late spring: A balloon borne observation. *Atmos. Environ.* 208, 48–60.
- Zhu, W., Xu, X.D., Zheng, J., Yan, P., Wang, Y.J., Cai, W.Y., 2018. The characteristics of abnormal wintertime pollution events in the Jing-Jin-Ji region and its relationships with meteorological factors. *Sci. Total Environ.* 626, 887–898.